Vibrational Spectroscopy of Small Matrix-Isolated Linear Carbon Cluster Anions

Jan Szczepanski, Scott Ekern, and Martin Vala*

Department of Chemistry and Center for Chemical Physics, University of Florida, Gainesville, Florida 32611

Received: October 17, 1996; In Final Form: January 2, 1997[⊗]

Carbon cluster anions have been generated, deposited in an argon matrix, and studied spectroscopically. A new method involving a dual laser beam-induced Ar plasma using Y or W metal and graphite targets is introduced for the efficient production of matrix-isolated carbon cluster anions. New bands found in the infrared spectra of the deposited plasma mixture have been assigned to asymmetric stretching modes of the C_3, C_5, C_6, C_7, and C_9 anions. Density functional theory calculations (B3LYP/6-31G* level) support the attribution of these bands to linear carbon cluster anions. Calculational results also indicate that reactions between linear anionic clusters and linear neutral clusters are highly exothermic and that aggregation between anions and even-membered neutrals are more highly exothermic than between anions and odd-membered neutrals. The anion infrared bands are found to be photosensitive at irradiation wavelengths shorter than a certain threshold value. These values are ca. 0.5 eV higher than the corresponding vertical detachment energies of the vapor phase C_n^- species. The possibility that longer chain carbon anions are present in the carbon-rich circumstellar envelopes of carbon stars is discussed.

I. Introduction

Carbon clusters have generated much current interest because of their involvement in soot formation, fullerenes, nanotubes, astrophysics, and material sciences.[1,2] Although the bulk of past work on carbon clusters has focused on neutral species, a much smaller quantity of work has been reported on negatively charged clusters. Carbon cluster anions have been studied using a variety of different experimental techniques including electronic absorption[3]and emission[4] in rare gas matrices, gas-phase anion photoelectron spectroscopy,[5−7] zero electron kinetic energy spectroscopy,[8,9] gas-phase ion chromatography,[10] and resonant multiphoton detachment spectroscopy.[11]

Recently, Gasyna, Andrews, and Schatz[12] reported on the electronic absorption spectra of the C_{60}^- fullerene ions prepared simultaneously with C_{60}^+ ions in a rare gas matrix. In mass spectroscopic work, Pergelis[13] used a cesium sputtering/ionization source to investigate the generation of various C_n^- species. The same ionization technique with mass selection and matrix isolation was employed by Maier and co-workers[3] to investigate the electronic absorption transitions of even-membered C_4^-−C_{20}^- carbon clusters in Ne matrices.

Several theoretical reports have appeared on different properties of the carbon cluster anions. Different spectroscopic parameters such as electronic transitions and electron affinities for the electronic ground states of small anionic carbon clusters were recently calculated by Raghavachari,[14,15] Watts and Bartlett,[16] Adamowicz,[17] and Schmatz and Botschwina[18] using high level ab initio approaches.

All work on negative carbon clusters up to 1989 has been thoroughly reviewed by Weltner and Van Zee.[19] Both experimental and theoretical work to the present have concluded that small carbon anions C_n^- ($n = 2-9$) are linear and that their neutral cluster parents have relatively high electron affinities (EA = 1.98−4.4 eV). Although symmetric mode frequencies have been reported for several anionic clusters,[4−6,11,18] no asymmetric mode frequencies have been reported to date.

II. Theoretical Procedures

All calculations have been carried out using the GAUSSIAN 94 program package.[20] The B3LYP exchange−correlation functional was used exclusively. This hybrid functional consists of the Lee−Yang−Parr correlation functional[21] and Becke's three-parameter exchange functional.[22] The exchange functional is a linear combination of the local density approximation, Becke's gradient correction,[23] and the "exact" Hartree−Fock exchange energy. This hybrid method has been shown to be more accurate than standard gradient-corrected methods.[24] The 6-31G* basis set was used throughout, since it has been found[25] to yield very similar geometries for neutral linear carbon clusters to the correlation consistent cc-pVDZ basis used by Martin, El-Yazal, and Francois.[26] Two general cluster geometries, linear and cyclic, were explored. For linear clusters, the shape was constrained to be linear and the bond lengths optimized. For the cyclic clusters, various geometries were investigated and the bond lengths and angles optimized within their respective point groups.

III. Experimental Procedures

Carbon clusters were formed in part during the vaporization of graphite (99.9995% ^{12}C purity) using a Q-switched Nd:YAG laser beam (1064 nm/532nm) and in part in the solid Ar matrix after the C_n/Ar gas streams were frozen on a cold (12 K) BaF_2 window (190 nm−13 μm range) cooled by a closed-cycle helium refrigerator (Displex APD Cryogenics). Argon (99.995% purity, Matheson) was used as the matrix gas.

In the present experiments attention was focused on the formation and spectral characteristics of negative ion carbon clusters. To form the clusters, electrons were added to the mixed C_n/Ar vapors converging on the cold window via either a low-energy electron beam or an Ar plasma. Negative cluster ions were partially extracted from the vaporization region by an electric field between an O-ring electrode situated close to the sample window and the cathode of the electron gun. The experimental setup is sketched in Figure 1. The electron gun has been described previously in detail.[27] The 532 nm laser beam was randomly vibrated across the surface of the graphite sample block to provide fresh carbon material for vaporization.

[⊗] Abstract published in *Advance ACS Abstracts,* February 1, 1997.

S1089-5639(96)03200-8 CCC: $14.00

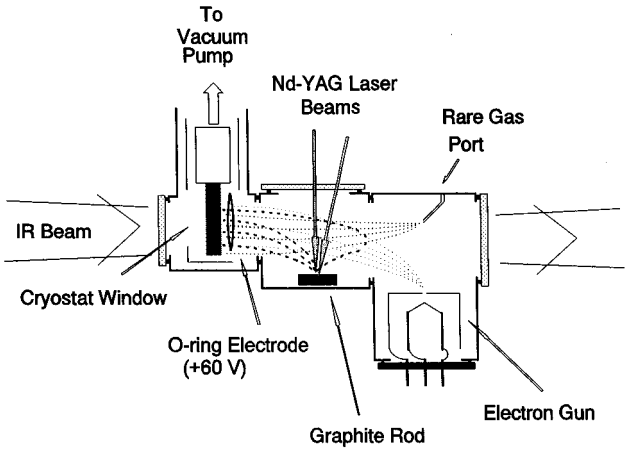

Figure 1. Cryostat deposition chamber used for preparation of C_n/C_n^-/Ar matrix. The electric field created between the −120 V filament of the electron gun, the +60 V O-ring electrode, and the grounded electron gun anode, cryostat shield, and shroud is used to extract some negative ions from the vaporization region. The O-ring electrode is mounted 0.5−1.0 cm from the BaF_2 window holder and is canted with respect to the cryostat window to prevent bombardment of negatively charged species on the matrix surface. The small piece of ^{39}Y or ^{74}W was pressed into the graphite surface and exposed to 1064 nm Nd:YAG laser radiation to create a blue metal/Ar plasma. The 532 nm second harmonic Nd:YAG laser beam was used to vaporize graphite material.

The O-ring control electrode indicated the intensity of the electron beam inside the deposition chamber. With a +60 V potential, the typical current collected by this electrode was 50 μA with only matrix gas flowing. During vaporization of graphite the current dropped to 20−30 μA. This drop was larger at higher concentrations of carbon in the C_n/Ar beam, indicating probable electron capture by the high electron affinity neutral carbon clusters.

Two different plasma methods were used to generate the anionic clusters: (1) focusing the 1064 nm/532 nm laser beam on a graphite target in the presence of Ar gas and electrons generated by the electron gun; (2) producing a metal/Ar plasma by focusing the 1064 nm laser beam, after dispersion from the 532 nm beam with a prism, onto a refractory metal target such as ^{39}Y or ^{74}W. The second harmonic beam was focused on the graphite surface located ca. 2−3 mm from the focal point of the plasma source. In this approach all ionization initiators (soft X-rays, vacuum UV photons, and electrons) may interact effectively with the C_n neutral clusters. The average O-ring electron current (measured at +60 V electrode potential) with the electron gun off was ca.15 μA. Although each of the above techniques produced carbon anions, the most efficient approach, as determined by the highest intensity ratio of C_n anion-to-neutral bands, was observed in approach 2.

Spectra of the carbon clusters in the IR region (7000−770 cm^{-1}) were recorded using a MIDAC FTIR spectrometer (0.7 cm^{-1} resolution). In the UV−visible−NIR ranges, a Cary 17 spectrophotometer was employed.

IV. Results

A. Theoretical Results. The goals of the present calculations were (1) to determine whether linear or cyclic geometries are more stable for the smaller carbon cluster anions, (2) to calculate the reaction energies between small linear carbon cluster anions and neutrals, and (3) to predict the vibrational frequencies and intensities for the different forms of carbon cluster anions to aid in assigning the observed infrared bands.

1. Stable Geometries. The optimized geometries using the B3LYP/6-31G* level theory for the linear cluster anions

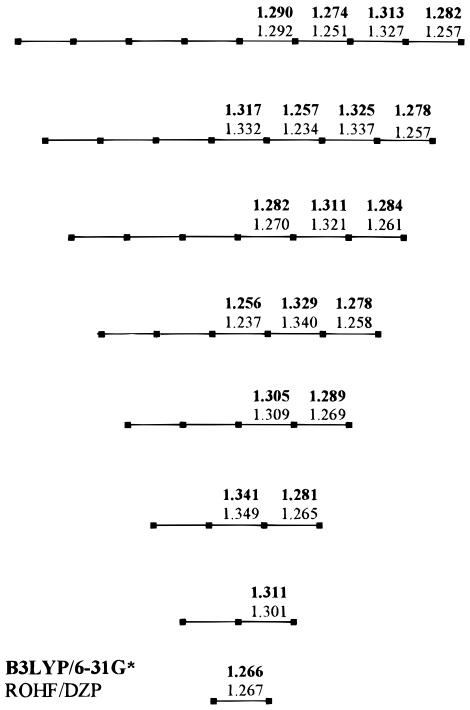

Figure 2. Linear carbon anion optimized geometries. Bond lengths in angstroms. B3LYP/6-31G* lengths are in bold type. ROHF/6-31G* lengths from ref 16 are in normal type.

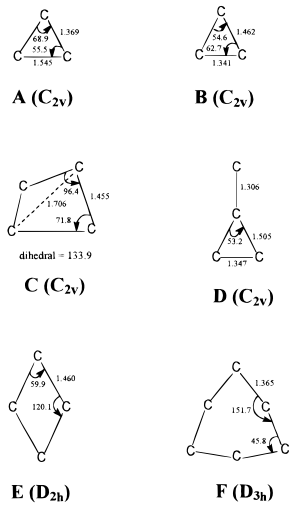

Figure 3. Optimized structures of all stable cyclic anion structures found at the B3LYP/6-31G* level of theory.

containing two to nine carbons are shown in Figure 2. The geometries are compared in the figure with the results of a ROHF/DZP study of carbon anions by Watts and Bartlett.[16] Both studies show geometries with a long/short bond alteration characteristic of an acetylenic structure, although the bond length differences are not as great as in a true acetylenic structure. The alteration found here is not as pronounced as in the Watts−Bartlett ROHF study. Nevertheless, the alteration agrees with the prediction that cumulenic neutral carbon clusters become more acetylenic as electrons are added.[16,28] With the exception of C_2^-, the average B3LYP-predicted bond length is (4.0−10.0) $\times 10^{-3}$ Å longer. The deviation from the average bond length is smaller than in the ROHF structures.

The geometries attempted for the cyclic C_3, C_4, and C_6 cluster anions are shown in Figure 3. Calculations were performed for several C_5^-, C_7^- ,C_8^-, and C_9^- cyclic structures, but no stable geometries were located. For cyclic C_3^-, an equilateral (D_{3h}) and two isosceles (C_{2v}) structures are possible. However,

no stable D_{3h} structure could be found at this level of theory. The C_{2v} structure **A** was found to be a stable minimum 14.4 kcal/mol higher in energy than the linear isomer. The other C_{2v} structure **B** was found to be a first-order saddle point whose energy-lowering vibrational motion led to the stable **A** form.

Five nonlinear structures were investigated for cyclic C_4^-, but only three minima (**C**, **D**, and **E**) were located (cf. Figure 3). Structure **C** is nonplanar and diamond-shaped (C_{2v} symmetry). The shortest distance between opposite carbons in the ring is 1.7 Å, indicating that no bond is formed across the ring. Its total energy is 57.7 kcal/mol greater than the linear C_4^- isomer. Structure **D** involves a three-membered ring and has C_{2v} symmetry. A Mulliken population analysis indicates that half the total charge resides on the terminal carbon on the "stem" of the ring. This structure has the lowest total energy of the three stable species studied, but its energy is still 37.7 kcal/mol higher than the linear isomer. Structure **E,** the next most stable isomer, has a planar diamond-shaped (D_{2h}) geometry and is predicted to lie 39.0 kcal/mol higher than the linear form. This difference is considerably larger than the difference between the corresponding neutral clusters (13.8 kcal/mol) predicted by Hutter, Lüthi, and Diederich.[29] Of the two remaining structures investigated that did not yield stable geometries, one was rectangular-shaped (D_{2h}) and found to be a third-order saddle point. Two of its imaginary modes were doubly degenerate and led to the planar diamond structure (**E**), while the third imaginary mode involved C−C bond rupture, creating a linear-like structure. The other unstable structure investigated had a pyramidal (C_{3v}) form. No stable minimum could be located for it.

Four six-membered ring structures were studied for cyclic C_6^-. Only two stationary points were found. Structure **F**, a planar ring having D_{3h} symmetry, is the lowest-energy cyclic C_6^- isomer and the only stable minimum found. Unlike their neutral C_6 counterparts, which are calculated to be nearly isoenergetic, structure **F** is predicted to be 35.8 kcal/mol higher in energy than its linear counterpart. The other stationary point located was a planar D_{6h} isomer, but this was found to be a second-order saddle point 59.9 kcal/mol higher in energy than the linear form. Its imaginary frequencies represent doubly degenerate motion, both of which lead to the D_{3h} minimum. Two other geometries were tested, neither of which yielded a stationary point. The first was a six-membered ring in a boat conformation, which consistently reverted to a D_{3h}-like structure. The second was an octahedral arrangement of carbon atoms for which no stable geometry was found. The overall conclusion that can be reached from the present calculations is that for the isomers calculated in both cyclic and linear forms, the linear structure is much more stable than the cyclic one.

2. Reaction Energies. Over 35 years ago Pitzer and Clementi calculated that reactions between neutral carbon clusters are strongly exothermic and should occur with no activation energy.[30] Since it has been observed here that annealing a matrix containing anionic and neutral carbon clusters leads to aggregation and the formation of larger cluster anions, it was of interest to determine whether such reactions are also predicted to be exothermic. Thus, DFT calculations (at the B3LYP/6-31G* level) of the reaction energies between small neutral and anionic carbon clusters were performed. The reactions studied were $C_n + C_m^- \rightarrow C_{n+m}^-$, where $n, m = 1-9$. For comparison with the reaction energy values for aggregation between small neutral clusters, calculations were also run at the same level of theory for these species. In both sets of calculations, linear clusters were chosen for study, since they appear to be the predominant structures for either neutral or anionic cluster species in matrices. The calculations involved finding the total energies for both reactant clusters and subtracting their sum from the total energy of the product cluster. These reaction energy values for neutral−neutral cluster aggregation are given in Table 1 for all possible reactant cluster combinations that yield products C_n with n from 2 to 9. The energies of reaction for all combinations of reactants are strongly exothermic, as found initially by Pitzer and Clementi. Figure 4 gives the analogous values for the reaction between anionic and neutral linear clusters to yield larger anionic chains. Zero-point energies were not included in the reaction energy values, since they represent only a small fraction (≤5%) of the total reaction energies. Several conclusions can be drawn from these results. First, for many cases the reaction energies between neutral and anionic clusters are more exothermic than their neutral−neutral counterparts. Second, aggregation reactions between anionic carbon clusters and even-membered neutral clusters are predicted to be 20−30% more exothermic than reactions between anionic clusters with odd-membered neutral clusters. These findings are consistent with our experimental findings (vide infra).

3. Vibrational Frequencies and Intensities. The major goal of this work was to determine the most probable geometries for carbon cluster anions and to predict their infrared spectra. These latter calculations have also been carried out using DFT theory at the B3LYP/6-31G* level for the vibrational frequencies and intensities of the linear ($n = 2-9$) and stable cyclic ($n =$ 3, 4, and 6) cluster anions. The results are displayed in Tables 2 and 3. Both symmetric and asymmetric mode frequencies are reported along with their calculated intensities.

TABLE 1: Energies of Reaction (kcal/mol) between Neutral Linear Carbon Chains Calculated at the B3LYP/6-31G* Level of Theory[a]

	$C(^3P)$	C_2	C_3	C_4
$C(^3P)$	−119.1			
$C_2(^1\Sigma_g^+)$	−199.2	−168.2		
$C_3(^1\Sigma_g^+)$	−88.1	−173.4	−104.7	
$C_4(^3\Sigma_g^-)$	−204.3	−215.8	−173.3	−223.6
$C_5(^1\Sigma_g^+)$	−130.5	−172.1	−107.5	−176.5
$C_6(^3\Sigma_g^-)$	−160.7	−176.0	−134.1	
$C_7(^1\Sigma_g^-)$	−134.5	−172.6		
$C_8(^3\Sigma_g^-)$	−157.2			

[a] Not zero-point corrected.

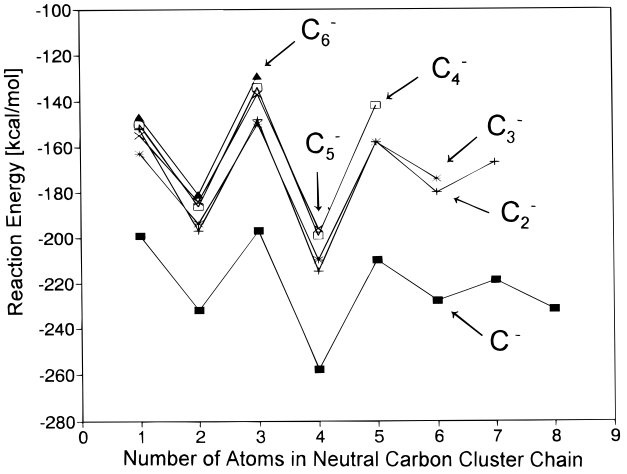

Figure 4. Plot of reaction energies (in kcal/mol) for reaction between anionic and neutral carbon clusters, calculated at the B3LYP/6-31G* level, vs the number of carbons in the neutral cluster chain. The neutral clusters were reacted with the anionic cluster given in the body of the graph to yield the resultant longer anionic chain: $C_n + C_m^- = C_{n+m}^-$ ($n = 1-8$, $m = 1-6$). The reactants and products are all in their ground electronic states. For electronic state descriptions of C_n and C_n^-, see Table 4.

TABLE 2: Vibrational Frequencies (Unscaled, cm^{-1}), IR Intensities (in Brackets, km/mol), Symmetries, and Rotational Constants (in Parentheses, GHz) for Linear Carbon Anions C_n ($n = 2-9$) in Their Electronic Ground States Calculated at the B3LYP/6-31G* Level

C_2^-	1872.7 [0] σ_g; (52.485338)
C_3^-	1772.1 [152] σ_u, 1201.9 [0] σ_g, 453.4 [28] π_u, 319.1 [40] π_u; (12.238791)
C_4^-	2112.7 [0] σ_g, 1785.2 [87] σ_u, 926.4 [0] σ_g, 605.4 [0] π_g, 533.1 [0] π_g, 265.5 [27] π_u, 241.5 [50] π_u; (4.946407)
C_5^-	1923.7 [0] σ_g, 1902.5 [855] σ_u, 1472.6 [23] σ_u, 777.2 [0] σ_g, 751.7 [0], 604.9 [8], 432.6 [0] π_g, 360.7 [0] π_g, 170.9 [35], 167.8 [24]; (2.495564)
C_6^-	2193.2 [0] σ_g, 2036.6 [726] σ_u, 1865.4 [0] σ_g, 1222.4 [1] σ_u, 810.5 [0], 774.7 [0], 657.9 [0] σ_g, 553.4 [3], 516.6 [12], 293.4 [0], 285.0 [0], 132.8 [24], 127.4 [30]; (1.432485)
C_7^-	2079.6 [0] σ_g, 1990.1 [157] σ_u, 1835.7 [2331] σ_u, 1608.7 [0] σ_g, 1089.9 [8] σ_u, 929.1 [2], 827.7 [3], 669.4 [0], 582.0 [0], 577.8 [0] σ_g, 416.3 [8] π_u, 367.4 [12] π_u, 226.4 [0], 221.1 [0], 94.6 [20], 93.6 [23]; (0.899969)
C_8^-	2174.8 [1563] σ_u, 2160.2 [0] σ_g, 2029.4 [0] σ_g, 1882.1 [512] σ_u, 1383.8 [0] σ_g, 983.5 [0], 964.4 [17] σ_u, 963.0 [0], 721.0 [1], 702.4 [0], 515.7 [0], 507.5 [0] σ_g, 489.5 [0], 306.6 [18], 303.5 [10], 187.6 [0], 181.7 [0], 74.6 [17], 73.5 [19]; (0.601110)
C_9^-	2147.5 [0] σ_g, 2083.1 [262] σ_u, 1941.1 [0] σ_g, 1814.9 [4201] σ_u, 1664.0 [728] σ_u, 1268.0 [0] σ_u, 1268.0 [0] σ_g, 1052.5 [3], 979.9 [1], 877.3 [132] σ_u, 806.8 [0], 732.7 [0], 603.4 [1], 542.5 [2], 547.4 [0] σ_g, 401.4 [0] π_g, 367.1 [0] π_g, 258.8 [16], 250.2 [11], 148.9 [0], 147.1 [0], 58.2 [14], 58.0 [15]; (0.422028)

TABLE 3: Vibrational Frequencies (cm^{-1}) and Intensities (in Brackets, km/mol) of the Cyclic Carbon Anions Calculated at the B3LYP/6-31G* Level

A	768.5 [0], 935.9 [53], 1558.9[14]
B	763.7i [617], 1154.0 [27], 1591.0 [1]
C	124.9 [0], 564.4 [8], 736.9 [105], 802.0 [9], 1247.0 [5], 1290.5 [1]
D	371.1 [1], 506.6 [4], 779.7 [50], 1334.5 [2], 1683.9 [1901], 1716.3 [0]
E	185.3 [0], 483.1 [35], 506.0 [39], 1006.0 [0], 1208.7 [6], 1324.3 [0]
F	451.9 [16], 552.6 [0], 552.6 [0], 598.6 [0], 600.3 [0], 600.3 [0], 919.9 [60], 920.2 [60], 1127.9 [0], 1245.5 [0], 1609.1 [275], 1609.1 [275]

TABLE 4: Comparison of Most Intense Calculated (Scaled by 0.95 Factor) and Experimental (Ar Matrix) Mode Frequencies (cm^{-1}) and Intensities (km/mol) for Linear (or Near Linear) Anion and Neutral Carbon Clusters[g]

anion				neutral				
cluster	ν_{calc}/cm^{-1} [a]	ν_{exp}/cm^{-1} [b]	$\nu_{calc} - \nu_{exp}$	cluster	ν_{calc}/cm^{-1} [c]	ν_{exp}/cm^{-1} [d]	$\nu_{calc} - \nu_{exp}$	mode
$C_2^-(^2\Sigma_g^+)$	1779.1 [0]	1777[e]	2.1	$C_2(^1\Sigma_g^+)$	1781.3 [0]	1854.7[f]	−73.4	$\nu_1(\sigma_g)$
$C_3^-(^2\Pi_g)$	1684.1 [152]	1721.8	−38.4	$C_3(^1\Sigma_g^+)$	2049.2 [772]	2038.9	10.3	$\nu_3(\sigma_u)$
$C_4^-(^2\Pi_g)$	1695.9 [87]			$C_4(^3\Sigma_g^-)$	1517.2 [291]	1543.4	−26.2	$\nu_3(\sigma_u)$
$C_5^-(^2\Pi_u)$	1807.4 [855]	1831.8	−24.4	$C_5(^1\Sigma_g^+)$	2155.6 [2539]	2164.1	−8.5	$\nu_3(\sigma_u)$
	1399.0 [23]				1423.1 [123]	1446.6	−23.5	$\nu_4(\sigma_u)$
$C_6^-(^2\Pi_u)$	1934.8 [726]	1936.7	−1.9	$C_6(^3\Sigma_g^-)$	1935.2 [1073]	1952.5	−17.5	$\nu_4(\sigma_u)$
	1161.3 [1]				1171.4 [95]	1197.3	−25.9	$\nu_5(\sigma_u)$
$C_7^-(^2\Pi_u)$	1890.6 [157]			$C_7(^1\Sigma_g^+)$	2145.1 [4652]	2128.0	17.1	$\nu_4(\sigma_u)$
	1743.9 [2331]	1734.8	9.1		1888.6 [1307]	1894.3	5.7	$\nu_5(\sigma_u)$
$C_8^-(^2\Pi_g)$	2066.1 [1563]			$C_8(^3\Sigma_g^-)$	2059.6 [1989]	2071.5	−11.9	$\nu_5(\sigma_u)$
	1788.0 [512]				1681.5 [737]	1710.5	−29.0	$\nu_6(\sigma_u)$
$C_9^-(^2\Pi_u)$	1978.9 [262]			$C_9(^1\Sigma_g^+)$	2106.2 [4077]	2078.0	28.1	$\nu_5(\sigma_u)$
	1724.2 [4201]	1686.7	37.5		2025.4 [6520]	1998.0	27.4	$\nu_6(\sigma_u)$
	1580.8 [728]	1583.3	−2.5		1586.5 [394]	1601.0	−14.5	$\nu_7(\sigma_u)$

[a] B3LYP/6−31 G* theory; this work. [b] This work. [c] B3LYP/CC-pVDZ theory; ref 26. [d] Reference 34 and references therein. [e] Reference 37. [f] Reference 38, gas phase. [g] The electronic ground-state symmetries are indicated. Intensities are given in brackets.

Schmatz and Botschwina have performed large-scale open-shell coupled cluster calculations on C_6^-, as well as other carbon anions.[18] They suggest that their frequency results are accurate to 2%. It is instructive to compare our B3LYP/6-31G* harmonic frequency calculations against the Schmatz−Botschwina results. Using the scaling factor of 0.95 (vide infra) for the B3LYP/6-31G* harmonic frequencies of the symmetrical modes of C_6^- (Table 2), we find ν_1 (scaled) = 2083.5 cm^{-1}, ν_2 (scaled) = 1772.1 cm^{-1}, and ν_3 (scaled) = 625 cm^{-1}; these values are all within the 2124 ± 42, 1790 ± 36, and 634 ± 13 cm^{-1} limits, respectively, predicted by Schmatz and Botschwina.

B. Experimental Results. *1. C_6^- Cluster*. In their mass selection/Ne matrix isolation study, Maier and co-workers reported the electronic absorption spectrum of C_6^-. Figure 5 (right side) shows an electronic absorption band system in an argon matrix that closely parallels the one observed by Maier and co-workers and assigned by them to the $^2\Pi_g - X^2\Pi_u$ electronic transition of C_6^-.[3] The O_0^0 electronic transition is shifted by 219 cm^{-1} compared to the transition in a Ne matrix.[3] A progression in the symmetrical ν_3 vibrational mode is observed. The ν_3 vibrational frequencies in the excited $^2\Pi_g$ state are practically independent of matrix or phase: $\nu_3 = 605$ cm^{-1} (Ar), 607 cm^{-1} (Ne),[3] and 602 cm^{-1} (gas).[11]

This band system (615.8 nm) is sensitive to bleaching by UV radiation. Since the concentration of positive ions sometimes also declines during photolysis (due to charge compensation by electrons liberated from anions), CCl_4 was used to check the charge of the deposited ions.[12] With CCl_4 added to the Ar matrix gas (0.1%), the electron beam and plasma create species such as Cl, CCl_2, CCl_3, and CCl_3^+. Because of their high electron affinities, these species act as electron traps in the matrix and thus compete with the C_n molecules for electrons.[27] With added CCl_4, the 615.8 nm system band intensities were considerably reduced compared to their intensities with no CCl_4 added. This is consistent with the assignment of these bands to a negative ionic species and is in agreement with their attribution to C_6^-.[3] This behavior is common to all the small negative carbon cluster species studied thus far.

A portion of the IR spectrum, recorded on the same sample matrix, is shown on the left-hand side of Figure 5. After 5 min photolysis (medium pressure 100 W Hg lamp, full spectral output) both the 615.8 nm and the 1936.7 cm^{-1} band intensities were reduced 20%. For all our experiments with small matrix concentrations of clusters, the intensity of the 1936.7 cm^{-1} band paralleled that of the 16 239 cm^{-1} band. We thus assign the 1936.7 cm^{-1} band also to C_6^-. It is the asymmetric stretching

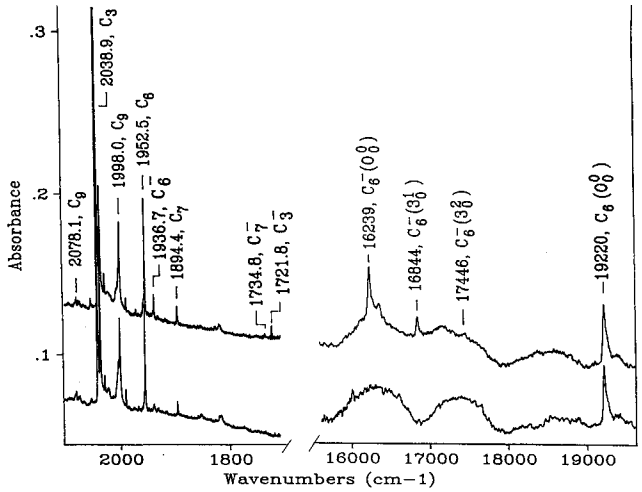

Figure 5. Vibrational (left) and electronic (right) spectra for C_n/C_n^- clusters in an Ar matrix deposited with the electron gun on (see Figure 1) recorded before photolysis (upper spectrum) and after 1/2 h photolysis using medium-pressure 100 W Hg lamp (full spectral output). The $^2\Pi_g - X^2\Pi_u$ electronic transition and the ν_4 vibrational mode frequency for C_6^- are marked. In this case only the electron beam was used as the ionization source (the 1064 nm laser beam was blocked).

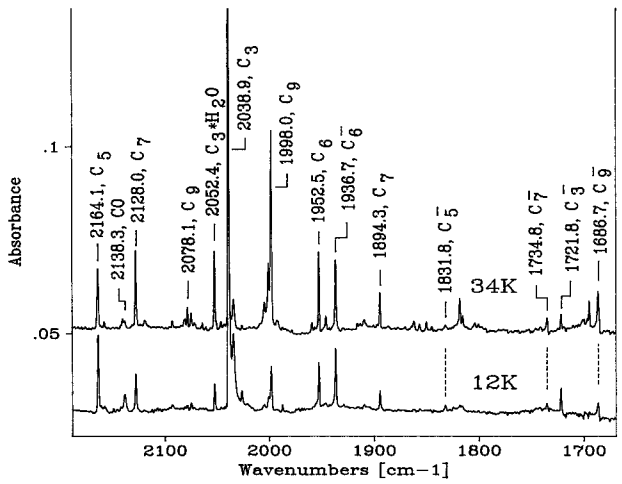

Figure 6. Part of the IR spectra of C_n/C_n^- in Ar deposited with the electron sources shown in Figure 1 active. The upper spectrum was recorded at 12 K after matrix annealing to 34 K.

mode of linear C_6^- (vide infra). For matrices prepared under conditions that favor formation of larger clusters, a new band centered at 1937 cm^{-1}, which is broader than the 1936.7 cm^{-1} band, appears. This new band is due to a species different from the C_6^- cluster.

The vertical electron detachment energy for gaseous C_6^- has been reported as 4.185 eV (296.2 nm).[6] By use of tunable monochromatized light (300 W Xe lamp with a 0.25 m monochromator), the 1936.7 cm^{-1} and 615.8 nm band intensities start declining after photolysis at wavelengths equal to or shorter than 265.5 nm (4.67 eV). We interpret this as the onset of the photodetachment threshold. The ca. 0.5 eV higher photodetachment energy for C_6^- in the matrix compared to the gas phase is due to the stabilization of C_6^- ions in the matrix cage.

Finally, density functional theory (DFT) calculations at the B3LYP/6-31G* level predict an intense asymmetric mode for linear C_6^- at 2036.6 cm^{-1} with an intensity of 726 km/mol (Table 2). Comparing this frequency to the experimental 1936.7 cm^{-1} value yields a scaling factor of 0.95. Martin, El-Yazal, and Francois, using DFT theory (B3LYP/cc-pVDZ level), have shown that this is a typical value for linear neutral C_n clusters.[26] Another infrared active band is predicted to appear at 1222.4 cm^{-1} (unscaled) with an intensity predicted to be 1 km/mol (Table 2) compared to 95 km/mol for the same mode in neutral linear C_6 (Table 4). This small intensity is presumably why this band is not seen in our C_6^- spectrum.

2. C_3^- Cluster. Neutral C_3 clusters are the most abundant species in laser-ablated, matrix-deposited neutral C_n/Ar samples. However, C_3^- anion bands were not easy to locate in the IR spectra of matrices prepared for anion studies. The calculated (B3LYP/6-31G*) frequency of the ν_3 mode for linear C_3^- is 1772.1 cm^{-1} (unscaled). However, the intensity of this band is small (152 km/mol), particularly compared to the intensity of the similar mode in neutral C_3 (772 km/mol , cf. Table 4). Nevertheless, a new band at 1721.8 cm^{-1} has been located that displays properties consistent with its assignment to C_3^-. These properties include the following. (1) Its frequency lies close to the theoretical value. A scaling factor of 0.97 is sufficient for an exact match. (2) The vertical electron detachment energy for C_3^- vapor has been determined to be 1.95 eV (635.8 nm).[5] By monitoring the intensity of the 1721.8 cm^{-1} band upon variable wavelength matrix photolysis, a photodetachment threshold energy of 2.19 eV (565 ± 5 nm) was determined. (3) The intensity of the 1721.8 cm^{-1} band declines during matrix annealing (Figure 6). This indicates that aggregation reactions between C_3^- and C_n neutrals are occurring more readily than reactions between smaller (than C_3) neutral and anion clusters that form C_3^- during matrix annealing. These observations lead to the tentative assignment of the 1721.8 cm^{-1} band to the asymmetric stretch of linear C_3^-.

3. C_5^- Cluster. DFT calculations predict (cf. Table 2) that the most intense IR active mode for C_5^- is the ν_3 asymmetric stretch mode at 1902.5 cm^{-1} (unscaled) with an intensity of 855 km/mol. Scaled by 0.95, ν_3 is expected around 1807 cm^{-1}. In the 1730−1930 cm^{-1} region, only one new band appears. It lies at 1831.8 cm^{-1} (Figure 6) and is photosensitive, i.e., it bleaches during photolysis using a medium-pressure Hg lamp. Thermal annealing of the matrix also produces a small bleaching effect on this band. This behavior might be expected for C_5^- based on the known intensity behavior for neutral C_5 and on the diffusion-controlled C_n aggregation model.[31]

4. C_7^- and C_9^- Clusters. Three additional bands at 1734.8, 1686.7, and 1583.3 cm^{-1} were observed in spectra recorded with one of the electron sources active. With CCl_4 added to the matrix gas, the intensity of these bands decreased substantially. Furthermore, these bands are photosensitive and *gain* in intensity during matrix annealing (Figures 6 and 7). The latter annealing behavior is contrary to what was observed for the smaller ($n = 3-6$) clusters. These observations suggest that the 1734.8, 1686.7, and 1583.3 cm^{-1} bands are due to negative ions whose sizes are larger than C_6^-. The intensity increase presumably arises because of aggregation of the smaller clusters to form larger ones.

Harmonic frequency calculations for linear C_7^- and C_9^- show that the most intense IR active band frequencies (unscaled/scaled) are, for C_7^-, $\nu_5 = 1835.7$ cm^{-1}/1743.9 cm^{-1} [2331 km/mol] and, for C_9^-, $\nu_6 = 1814.9$ cm^{-1}/1724.2 cm^{-1} [4201 km/mol], $\nu_7 = 1664.0$ cm^{-1}/1580.8 cm^{-1} [728 km/mol]. The +9.1, +37.5, and −2.5 cm^{-1} deviations for C_7^- and C_9^- are acceptable, since the common scaling factor (0.95) was transferred from C_6^- and used unchanged (cf. Table 4 for comparison of energy shifts for neutrals). We thus tentatively assign the 1734.8 cm^{-1} band to the ν_5 asymmetric stretch of C_7^- and the 1686.7 and 1583.3 cm^{-1} bands (in Ar) to the ν_6 and ν_7 asymmetric stretch modes of C_9^-, respectively.

The calculated frequencies for the cyclic structures (cf. Table 3) lead to the conclusion that cyclic isomers could not be the

carriers of the observed anionic bands. All IR active bands for the cyclic structures are predicted to lie below 1700 cm^{-1}, although the 1683.9 cm^{-1} band of the C_4^- isomer **D** does lie near the range of the experimental bands. This is also the only band that has intensity comparable to those of the linear anions (1901 km/mol). Thus, of the cyclic isomers, **D** is probably the one most likely to be observed. However, it is calculated to be 1.5 eV less stable than the linear isomer, so its nondetection is understandable.

V. Discussion

Three different methods of anionic carbon cluster formation were used in these studies. All negative ion bands reported were observed with each of the three methods, though not with the same intensities. The most promising and convenient ionization source for matrix isolation ion spectroscopy is the plasma formed by Nd:YAG laser irradiaion of ^{39}Y or ^{74}W and graphite. By use of two dispersed Nd:YAG laser beams, one (1064 nm) for ionization and the second (532 nm) for vaporization of graphite, there is ample opportunity for interaction between the plasma-producing pulse and the C_n beam pulse. The plasma source most probably emits electrons, UV photons, and X-radiation. The X-radiation from this type of source has been found to have a broad energetic spectrum with a maximum at 30 nm.[32] The UV photons and X-radiation can be expected to both ionize and electronically excite both the C_n and Ar species in the vapor phase. Subsequently, carbon chain anions may be formed from the free electrons in the plasma. We note that with the present experimental setup no new species such as C_nY_k or C_nW_l were observed in the 4000−750 cm^{-1} scanned region. All bands reported here as C_n^- bands were observed in the "pure" C_n/Ar/electron beam matrix experiments as well. Furthermore, all the IR bands assigned here to linear C_n^- carbon clusters were observed only during experiments in which one of the ionization sources was active.

Taking into account the calculated intensities (Tables 2 and 4) and the ratios of absorbancies from the spectrum in Figure 6 (lower), we can estimate the percentage of anion $[C_n^-]$ concentration relative to the sum of the neutral $[C_n]$ and anion $[C_n^-]$ concentrations. They are $[C_3^-]/([C_3] + [C_3^-]) = 19.9\%$, $[C_5^-]/([C_5] + [C_5^-]) = 17.3\%$, $[C_6^-]/([C_6] + [C_6^-]) = 64.8\%$, $[C_7^-]/([C_7] + [C_7^-]) = 14.5\%$, and $[C_9^-]/([C_9] + [C_9^-]) = 30.5\%$. The highest concentration percentage occurs for the even C_6^- cluster. The formation of even linear carbon anions is preferred, as can be seen in the reaction energy plots (Figure 4) as well as from the electron affinities for C_n.[5] From ref 5 it is clear that the electron affinities for small, even C_n clusters are ca. 1 eV higher than for small, odd clusters. From Figure 4 we can also see that aggregation reactions involving the anions and neutral linear clusters are all highly exothermic. This type of reaction will be controlled by diffusion of the carbon species in solid Ar. This explains the changes in the experimental band intensities during matrix annealing in a manner similar to that for neutrals[31] (cf. Figures 6 and 7).

The sample/matrix typified by the spectrum in Figure 6 was deposited with ca. 4×10^4 laser shots. Assuming the theoretical value of the C_6^- 1936.7 cm^{-1} band intensity of 726 km/mol is correct (Table 2), we can estimate the number of C_6^- ions per laser shot formed, trapped, and stabilized in the matrix. For a 100 μm thick matrix, 1 cm cryostat window radius, and a 1.3 cm^{-1} fwhm bandwidth, an average number of 6×10^{10} C_6^- ions per laser pulse were accumulated.

The existence of negatively charged carbon clusters in the matrix requires the presence of positively charged species for charge balance.[33] In searching for positive ion species in the IR, several were located: 903.4 cm^{-1} due to ArH^+ and 1036.6 cm^{-1} due to CCl_3^+ recorded during C_n/Ar/CCl_4/electron beam experiments. It seems reasonable to expect that, in addition to the anions, there are many different carbon cluster *cations* in the matrix (whose band intensities may fall below the base line noise) and also Ar^+ ions (which are IR silent).

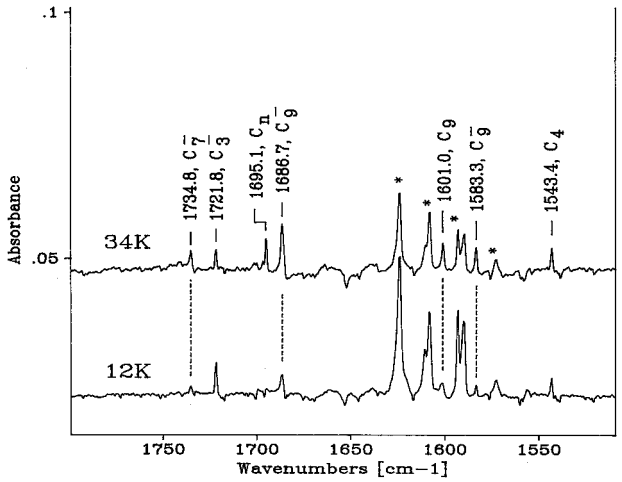

Figure 7. C_n/C_n^-/Ar infrared spectra in the bending region of water before annealing (lower spectrum) and after annealing to 34 K (upper spectrum). The water bands are marked by stars. Negative peaks in the spectrum are due to uncompensated rotational bands of water in the gas phase.

Vibrational band positions have been found in this work for all the small linear carbon cluster anions ($3 \le n \le 9$), with the exception of C_4^- and C_8^-. It is thus pertinent to ask why they have not been observed. Table 2 shows that for C_4^-, the most intense band, the ν_3 asymmetric stretching mode, is expected at 1695.9 cm^{-1} (scaled), but that its predicted intensity is only 87 km/mol. By comparison of this to the 291 km/mol intensity for the same mode of neutral C_4 (cf. Table 4) and assuming a 20% concentration for C_4^- vs C_4, based on the 3.5×10^{-3} absorbance for the ν_3 mode of C_4 (Figure 4), the expected absorbance for ν_3 of C_4^- is only 2×10^{-4}. This is below the noise level in the 1700 cm^{-1} region. For linear C_8^-, the most intense band, the ν_5 mode, should appear at 2066.1 cm^{-1} (scaled) with a 1563 km/mol intensity. This is ca. 20% smaller than for the ν_5 mode of neutral C_8 (Table 4; the 2071.5 and 1710.5 cm^{-1} bands have recently been assigned to the ν_5 and ν_6 modes of C_8 (in Ar)[34]). But the concentration of C_8, and undoubtedly C_8^- as well, is too small in our matrix to observe either cluster.

Comparison of the most intense IR active modes for anionic and neutral clusters (Table 4) shows that generally vibrational frequencies for the anions are shifted to lower energies (except for C_8^-). The drastic changes in band intensities and in the distribution of intensities over particular modes of the carbon anions should be noted. For example, the intensities of the most intense IR modes for C_3^-, C_4^-, and C_5^- decrease 3−5 times compared to the intensitites of the same modes of the neutrals. The intensities of the ν_4 and ν_5 modes of C_7^- are switched with respect to the intensities of the analogous modes of neutral C_7. These frequency and intensity changes are due to fact that carbon cluster anions have a different CC bond character. As a number of theoretical studies have shown[16−18] and as we can see from this study, there is an alternation in the bond length for all linear carbon anions. Thus, although the neutral linear clusters are cumulenic, the anionic linear clusters adopt a more acetylenic structure.

The high yield of the C_n^- species generated in the present study suggests the possibility that this type of species may occur in the circumstellar envelopes surrounding mass-losing carbon

stars, such as asymptotic giant branch (AGB) type carbon stars. These stars, whose carbon concentrations are far greater than their oxygen concentrations, are the main source of carbon and carbon-bearing species in the interstellar medium (ISM).[35] The effects of photodestruction are expected to be smaller for the longer carbon anions because they have higher vertical electron detachment energies.[16] In fact, we have just recently found that anionic even-membered carbon chains from C_{16}^- and longer are photostable under UV irradiation in an Ar matrix.[36] This observation is in agreement with an earlier study reported for even carbon C_n^- clusters in a Ne matrix.[3] We speculate that in the circumstellar envelopes there may be a dynamic equilibrium between the creative processes forming C_n^- clusters (such as electron capture and/or anion−neutral reactions) and the photolytic processes destroying the clusters (such as electron photodetachment and photodissociation). If true, the presence of negative linear carbon clusters in the ISM is conceivable.

Acknowledgment. The authors gratefully acknowledge the National Aeronautics and Space Admininistration for its support of this research.

References and Notes

(1) Rinzler, A. G.; Hafner, J.; Nikolaev, P.; Lou, L.; Kim, S. G.; Tomanek, D.; Nordlander, P.; Colbert, D. T.; Smalley, R. E. *Science* **1995**, *269*, 1550, and references therein.

(2) Herbig, G. H. *Annu. Rev. Astron. Astrophys*. **1995**, *33*, 19, and references therein.

(3) Forney, D.; Freivogel, P.; Jacobi, M.; Lessen, D.; Maier, J. P. *J. Chem. Phys*. **1995**, *103*, 43. Freivogel, P.; Fulara, J.; Jacobi, M.; Forney, D.; Maier, J. P. *J. Chem. Phys*. **1995**, *103*, 54.

(4) Schafer, M.; Grutter, M.; Fulara, J.; Forney, D.; Freivogel, P.; Maier, J.P.; *Chem. Phys. Lett*. **1996**, *260*, 406.

(5) Yang, S.; Taylor, K. J.; Craycraft, M. J.; Conceicao, J.; Pettiette, C. L.; Cheshnovsky, O.; Smalley, R. E. *Chem. Phys. Lett*. **1988**, *144*, 431.

(6) Arnold, D. W.; Bradforth, S. E.; Kitsopoulos, T. N.; Neumark, D. M. *J. Chem. Phys*. **1991**, *95*, 8753.

(7) Handshuh, H.; Gantefor, G.; Kessler, B.; Bechthold, P. S.; Eberhardt, W. *Phys. Rev. Lett*. **1995**, *77*, 1095.

(8) Kitopoulos, T. N.; Chick, C. J.; Zhao, Y.; Neumark, D. M. *J. Chem. Phys*. **1991**, *95*, 5479.

(9) Arnold, C. C.; Zhao, Y.; Kitopoulos, T. N.; Neumark, D. M. *J. Chem. Phys*. **1992**, *97*, 6121.

(10) Helden, G.; Gotts, N. G.; Bowers, M. T. *Nature* **1993**, *363*, 60.

(11) Zhao, Y.; deBeer, E.; Xu, C.; Taylor, T.; Neumark, D. M. *J. Chem. Phys*. **1996**, *105*, 4905.

(12) Gasyna, Z.; Andrews, L.; Schatz, P. N. *J. Phys. Chem.* **1992**, *96*, 1525.

(13) Pargellis, A. N. *J. Chem. Phys*. **1990**, *93*, 2099.

(14) Raghavachari, K. *Z. Phys. D* **1989**, *12*, 61.

(15) Raghavachari, K. *Chem. Phys. Lett*. **1990**, *171*, 249.

(16) Watts, J. D.; Bartlett, R. J. *J. Chem. Phys*. **1992**, *97*, 3445.

(17) Adamowicz, L. *Chem. Phys. Lett*. **1991**, *182*, 45.

(18) Schmatz, S.; Botschwina, P. *Chem. Phys. Lett*. **1995**, *235*, 8; *Ibid*. **1995**, *245*, 136; *Int. J. Mass Spectrom. Ion Processes* **1995**, *149/150*, 621.

(19) Weltner, W., Jr.; Van Zee, R. J. *Chem. Rev*. **1989**, *89*, 1713.

(20) Frisch, M. J.; Trucks, G. W.; Schlegel, H. B.; Gill, P. M.; Johnson, B. G.; Robb, M. A.; Cheeseman, J. R.; Keith, T.; Petersson, G. A.; Montgomery, J. A.; Raghavachari, K.; Al-Laham, M. A.; Zakrzewski, V. G.; Ortiz, J. V.; Foresman, J. B.; Peng, C. Y.; Ayala, P. Y.; Chen, W.; Wong, M. W.; Andres, J. L.; Replogle, E. S.; Gomperts, R.; Martin, R. L.; Fox, D. J.; Binkley, J. S.; Defrees, D. J.; Baker, J.; Stewart, J. P.; Head-Gordon, M.; Gonzalez, C.; Pople, J. A. *GAUSSIAN 94*, Revision B.2; Gausssian, Inc.: Pittsburgh, PA, 1995.

(21) Lee, C.; Yang, W.; Parr, R. *Phys. Rev. B* **1988**, *37*, 785.

(22) Becke, A. D. *J. Chem. Phys*. **1993**, *98*, 5648.

(23) Becke, A. D. *J. Chem. Phys*. **1988**, *88*, 1053.

(24) Barone, V.; Adamo, C.; Mele, F. *Chem. Phys. Lett*. **1996**, *249*, 290.

(25) Ekern, S. P.; Szczepanski, J.; Vala, M. Unpublished results.

(26) Martin, J. M. L.; El-Yazal, J.; Francois, J. *Chem. Phys. Lett*. **1995**, *242*, 570.

(27) Szczepanski, J.; Vala, M.; Talbi, D.; Parisel, O.; Ellinger, Y. *J. Chem. Phys*. **1993**, *98*, 4494.

(28) Watts, J. D.; Gauss, J.; Stanton, J. F.; Bartlett, R. *J. Chem. Phys*. **1992**, *97*, 8372.

(29) Hutter, J.; Luthi, H. P.; Diederich, F. *J. Am. Chem. Soc*. **1994**, *116*, 750.

(30) Pitzer, K. S.; Clementi, E. *J. Am. Chem. Soc*. **1959**, *81*, 4477.

(31) Szczepanski, J.; Pellow, R.; Vala, M. *Z. Naturforsch*. **1992**, *A47*, 595.

(32) Wellegehausen, B.; Hube, M.; Jin, F. *Appl. Phys*. **1989**, *B49*, 173.

(33) Godbout, J. T.; Halasinski, T. M.; Leroi, G. E.; Allison, J. *J. Phys. Chem*. **1996**, *100*, 2892.

(34) Szczepanski, J.; Ekern, S.; Chapo, C.; Vala, M. *Chem. Phys*. **1996**, *210*, 359.

(35) Jura, M.; Kleinmann, S. G. *Astrophys. J*. **1989**, *336*, 924.

(36) Vala, M.; Ekern, S.; Szczepanski, J. To be published.

(37) Bondybey, V.; Nibler, J. W. *J. Chem. Phys*. **1972**, *56*, 4719.

(38) Hubert, K. P.; Herzberg, G. *Constants of Diatomic Molecules*; Van Nostrand Reinhold: New York, 1979.